machines

MDPI

Article

Human–Machine Shared Steering Control for Vehicle Lane Changing Using Adaptive Game Strategy

Xiaodong Wu [1,*], Chengrui Su [2] and Liang Yan [2]

[1] School of Mechanical Engineering, Shanghai Jiao Tong University, 800 Dongchuan Road, Shanghai 200240, China
[2] Institute of Intelligent Vehicle, Shanghai Jiao Tong University, 800 Dongchuan Road, Shanghai 200240, China
* Correspondence: xiaodongwu@sjtu.edu.cn

Abstract: Human–machine shared control of intelligent vehicles is considered an important technology during the industrial application of autonomous driving systems. Among the engineering practices in driver assistance systems, shared steering control is one of the important applications for the human–machine interaction. However, how to deal with human–machine conflicts during emergency scenarios is the main challenge for the controller's design. Most shared control approaches usually generate machine-oriented results without enough attention to the driver's reaction. By taking the human driver and machine system as two intelligent agents, this paper proposes a game-based control scheme to achieve a dynamic authority allocation during the lane changing maneuver. Based on the modeling of predicted trajectories of the human driver, a human-intention-based shared steering control is designed to achieve dynamic Nash game equilibrium. Moreover, a human-oriented shared steering mechanism is employed to not only benefit from automated machine assistance, but also make full play of human contributions. Using quantitative comparative analysis in lane changing scenarios with different human–machine conflicts, a better performance by considering both driving comfort and safety is achieved.

Keywords: human–machine interaction; shared control; game control; lane changing maneuver

check for updates

Citation: Wu, X.; Su, C.; Yan, L. Human–Machine Shared Steering Control for Vehicle Lane Changing Using Adaptive Game Strategy. *Machines* **2023**, *11*, 838. https://doi.org/10.3390/machines11080838

Academic Editor: Angelica Reyes

Received: 24 June 2023
Revised: 14 August 2023
Accepted: 16 August 2023
Published: 17 August 2023

Copyright: © 2023 by the authors. Licensee MDPI, Basel, Switzerland. This article is an open access article distributed under the terms and conditions of the Creative Commons Attribution (CC BY) license (https://creativecommons.org/licenses/by/4.0/).

1. Introduction

With the development of automated driving technology, intelligent vehicles have received growing attention to improve driving safety and reduce human drivers' workload in recent years. However, there are still many challenges with the existing technologies to achieve fully driverless vehicles in complex environments [1]. Based on the SAE standard, human-in-the-loop control is still the main technical approach for $L0 \sim L3$ intelligent vehicles before $L4 \sim L5$ fully automated driving. The human–machine interaction technology is a kind of advanced driving-assistance system (ADAS) which can be used to improve active safety, reduce driver workload [2], even reduce energy consumption [3]. A shared control concept through the combination of manual mode and automated mode offers a new solution to solve the control authority between the human driver and the machine's systems [4,5].

During the engineering practices of ADASs, steering control on the vehicle is usually implemented with traded control mode and shared control mode [6]. Traded control mode means that the human driver is considered as the independent driving input, and the machine system is used to enhance the driver's perception and control ability. Human–machine interaction is a kind of master–slave relationship in this kind of steering control. Shared control mode takes the human driver and the machine system as two parallel control inputs [7]. Shared steering control is one of the important applications for the lange change maneuver for intelligent vehicles. Based on the lane changing situations, the control authority is switched between the two intelligent agents. The two intelligent

agents possess the control authority simultaneously, and coupling results are generated according to a certain principle [8].

The shared steering control in this paper is studied on a steer-by-wire (SBW) system with an uncoupled mechanism. The modeling of human–machine cooperative steering control is based on the decoupling characteristic. There are two key issues during the design of shared steering control. The first is how to integrate different inputs from two lane-changing participants. From the previous literature, most studies conducted the integration of driver and machine steering input through an angle-based sharing method. The control authority is distributed by a weight coefficient to couple inputs from the human driver and the machine system [9,10]. The shared steering strategy is designed by mapping the path tacking error onto the guiding steering angle. However, the angle-based sharing method usually generates unexpected steering results, thus leading to a confused sense for the human handling reaction [11]. To build a feedback mechanism during human–machine interactions, this paper employs a torque-based sharing method to avoid possible violent steering guidance from the assistance system. The torque-based human–machine cooperative control allows the driver to remain in the control loop, and can achieve relatively smooth authority distribution [12,13]. This kind of approach is also studied as a haptic shared control strategy.

The second issue is how to deal with the conflict between human input and machine assistance. A variety of model-based human–machine cooperative methods have been designed for the shared steering controller, of which the model predictive control (MPC) [14,15] and linear quadratic regulator (LQR) [16,17] have been used to solve the human–machine interaction in trajectory tracking control. The model-based approaches with static numerical derivation are difficult to describe the dynamic characteristic of the human driver reaction. To describe and address conflicts between human and machine, game theory is an effective method to apply to such interactive decision-making systems. The game-based approach makes the human and machine drive the vehicle in parallel, where the choice of steering action of each control agent depends on that of the other [18]. For the research of human–machine multi-agent systems, and given the advantages of game equilibrium strategy, this paper investigates shared steering control from a dynamic game theory approach.

Since steering systems may be either mechanically coupled or uncoupled, the game-theory-based controllers in previous studies were designed to receive considerable attention for both coupled and uncoupled shared control. In coupled shared steering control, the driver and the machine interact through a motorized steering wheel that is mechanically coupled to the vehicle tires. By considering a torque-overlay-based shared control framework, the allocation of the steering effort is calculated by the game equilibrium between the driver and machine assistance [17,19,20]. In uncoupled shared steering control, the driver controls the vehicle indirectly through an uncoupled steering system, such as steer-by-wire (SBW) or active front steering (AFS). Non-cooperative approaches using game theories have been designed to study the interaction between the driver and an AFS system from the theoretical point of view, using the LQR and MPC techniques for modeling and control [21–24]. The main issue of coupled shared steering control is the torque conflicts due to the different intentions of the human driver and the machine system, while uncoupled control may cause the driver to experience a lack of control when the machine system does not exactly follow the driver's intention [25].

The human–machine interaction should be modeled to simultaneously enhance driving safety and reduce the degree of conflicts during shared steering control. Most of these game-based approaches are designed using the complete information hypothesis, where the game players can achieve full information from each other. The interaction of human and machine is conducted to follow a predefined principle during the conflict, and the control authority is assigned by an absolute trusting of the machine system. However, in emergency lane-changing conditions with incomplete information, these kinds of game-based schemes usually generate machine-oriented shared results without enough attention to the driver's

reaction. To solve this issue, in the game-based modeling of human–machine interactions, the weighting matrix of optimal control inputs should be adaptive to describe this kind of human-oriented relationship, which has not been emphasized in previous studies.

In order to address the authority distribution during lane changing conditions, the intention of the human driver should be considered in the shared steering control. The attention of the human driver can be easily focused again after being reminded, but the decision of machine intelligence is limited to the performance of the sensory system. In this paper, a long short-term memory (LSTM) network is employed as the driver's-intent recognition model. This paper designs a steering torque cooperative framework for lane changing by using Nash equilibrium game theory. In the proposed framework, the shared control not only benefits from automated machine assistance, but also make full play of human contributions. Based on the experimental analysis in a hardware-in-the-loop (HIL) platform, the proposed strategy is verified by comparing the performance with the game algorithms from the existing literature. The main contributions of this paper are summarized as follows.

(1) An adaptive parameter-adjustment scheme is designed to achieve dynamic Nash equilibrium during shared steering control. By dynamically changing the authority distribution coefficient, a smooth resolution of human–machine steering conflicts to improve both driving comfort and safety can be achieved.

(2) A human-oriented shared steering control is employed to establish a flexible interaction mechanism. Based on the conflict degree of the steering torque, the machine system can reduce inappropriate assistance to follow the specific intention of the human driver. The proposed adaptive game approach can avoid single machine-oriented control results, in which the driver can play a dominant role after the recovery of human attention.

This paper is organized as follows. Section 2 gives a brief introduction of the system architecture, and the modeling of driving paths from human and machine intelligence are investigated, respectively. Section 3 presents the establishment of a shared steering control algorithm using a game-based theory, and the interaction between the human driver and machine system is resolved by a series of non-cooperative Nash games. Section 4 offers a detailed description of the experimental verification for the proposed control strategy in the self-developed HIL experiments. The conclusion of the human–machine shared steering control for vehicles in this paper is summarized in Section 5.

2. Modeling of Human–Machine System

The modeling of the human–machine system was designed by combining a single-track vehicle dynamics model with a steer-by-wire (SBW) system. Compared with the traditional mechanical steering system, the SBW system removed the mechanical linkage between the steering column and steering actuator [26]. In this paper, human–machine shared steering control is investigated by using the decoupling characteristics of SBW systems. Based on the numerical models of both the human driver and machine system, the target paths from two participants can be generated, respectively. The shared steering motion of the vehicle is a dynamic game process between the human driver and machine system.

2.1. System Architecture

The system architecture of the shared steering control frame is shown in Figure 1. By considering the shared control as a linear-discretized system with time sequence k, here $L_1(k)$ and $L_2(k)$ denote the target trajectories of the machine system and human driver, respectively; $\tau_1(k)$ and $\tau_2(k)$ represent the steering torque generated from the machine and driver, respectively; $x(k)$ is the state parameters of the controlled vehicle dynamics, which are discretized as a time sequence. The interaction of human–machine shared control is coupled by steering torque from each other, and the vehicle is driven by the driver and machine simultaneously.

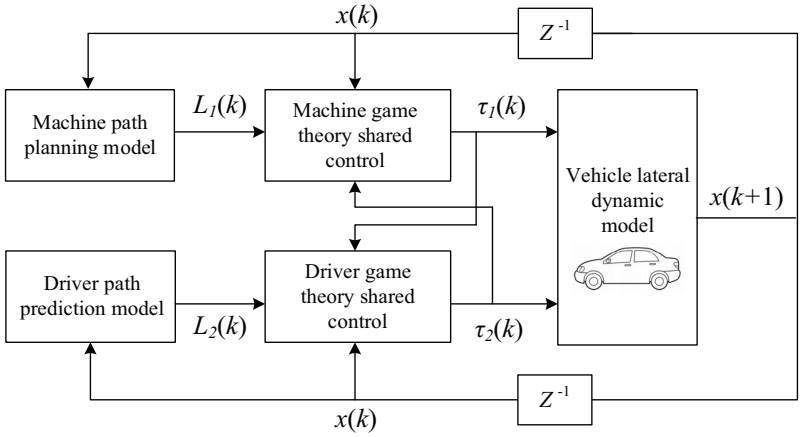

Figure 1. Architecture of the shared control model with game theory.

The human driver and machine system generate the optimal driving actions according to the respective target, which can be considered as a certain principle of game-based equilibrium. During lange changing control, the game-based equilibrium usually generates a compromise result to balance the different requirements of the two participants, which may not satisfy traffic regulations. For example, the vehicle should be driven in the middle of the lane according to traffic rules, but a neutral trajectory of the game result to make the vehicle run along the lane line between two traffic lanes would be unreasonable [8]. It is also difficult for the machine system to discover its inappropriate decision under complex situations, such as the driverless dilemma in [27].

To solve the above issue, game-based shared steering control can be designed as a human-oriented mode. This means the shared principle has the ability to return control authority to the driver after the recovery of human attention. This paper employs a torque-based shared steering control to establish a flexible human–machine interaction mechanism. When a conflict occurs, the machine will generate a reaction torque on the steering handwheel to correct the driver's action. The conflict can be resolved if the driver accepts the proposed action of the machine. However, if the driver does not accept the assisted machine action, the driver will increase the steering torque to maintain the original operation. Here, the accumulation of dot products between the steering torques from the two participants is employed to recognize the driving attention of the human. More details of the control algorithm will be given in the following section.

2.2. Vehicle Lateral Dynamics

In order to analyze the shared steering control, an integrated numerical model was considered by combining the vehicle dynamics with the steering system. To simplify the modeling of the vehicle's motion, the single-track dynamics model shown in Figure 2 was designed. With an assumption of constant longitudinal motion speed in the lane changing maneuver, the lateral dynamics equations of the vehicle can be expressed as

$$\begin{cases} m_c\left(\dot{v}_y + v_x\dot{\varphi}\right) = F_f + F_r \\ J_c\ddot{\varphi} = l_f F_r - l_r F_r \\ \dot{e}_\varphi = \dot{\varphi} - \kappa \\ \dot{e}_y = v_x \sin e_\varphi + v_y \cos e_\varphi \\ \dot{s} = \frac{1}{1-\kappa e_y}\left(v_x \cos e_\varphi - v_y \sin e_\varphi\right) \end{cases} \tag{1}$$

where m_c is the mass of the vehicle; J_c is the yaw moment of inertia of the vehicle; v_x and v_y are its longitudinal and lateral speeds; φ is the yaw angle of the vehicle relative to the road; l_f and l_r are the distances between the front/rear axle and the center of gravity of the vehicle, respectively; F_f and F_r are the lateral forces generated by the front and rear tires; e_φ

is the included angle between the vehicle heading direction and the road center tangent; e_y is the lateral offset between the vehicle and the road's center line; κ is the road curvature; and $\dot{s}$ is the component speed along the road direction.

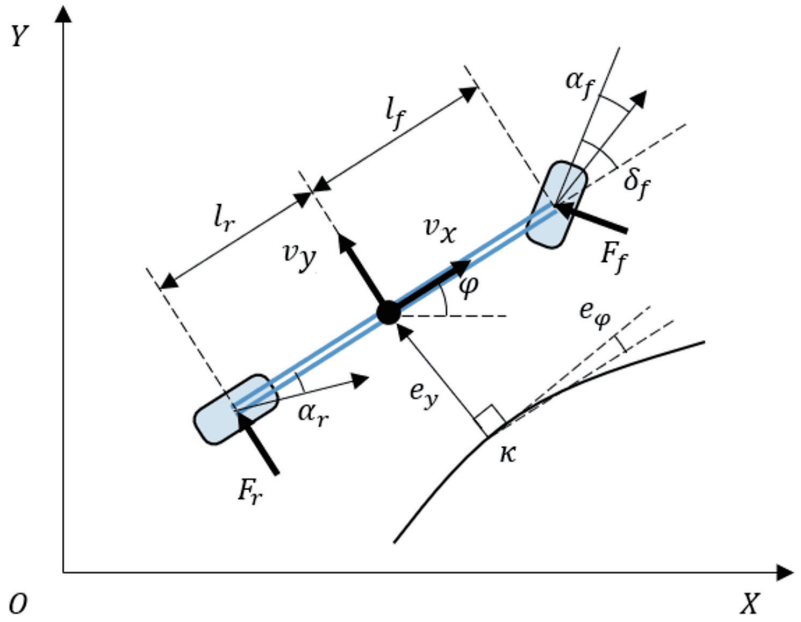

Figure 2. Vehicle single-track dynamics model.

If the vehicle is driving on a road with little curvature ($\kappa \approx 0$), the included angle between the vehicle heading direction and the road center tangent e_φ is assumed to keep in a relatively small range. Thus, parts of the lateral dynamics equations of the vehicle in Equation (1) can be rewritten as

$$\begin{cases} \dot{e}_\varphi = \dot{\varphi} \\ \dot{e}_y = v_x e_\varphi + v_y \\ \dot{s} = v_x - v_y e_\varphi \end{cases} \tag{2}$$

Based on the above assumption of a small steering angle, the relationship between the slip angle and the lateral forces generated by the vehicle tires can be considered as an approximate linear relation. Thus, a linear tire model can be employed to approximately calculate the lateral force generated by the front and rear tires:

$$\begin{cases} F_f = 2C_f\left(\dfrac{v_y + l_f\dot{\varphi}}{v_x} - \delta_f\right) \\ F_r = 2C_r\dfrac{v_y - l_r\dot{\varphi}}{v_x} \end{cases} \tag{3}$$

where C_f and C_r represent the cornering stiffness of a single front tire or rear tire under its static load, and δ_f is the front wheel steering angle.

According to the previous study of steering systems [26], the handwheel system can be regarded as a rigid body. During shared steering control, the modeling of the handwheel module is considered as a one degree-of-freedom system. Based on Newton's laws, the elements on the handwheel module are represented by its total moments of inertia and viscous friction coefficients. Based on this assumption, the steering dynamics function can be described as a second-order system, and the differential equation is given as

$$J_{SW}\ddot{\theta}_{SW} = \tau_1 + \tau_2 - \tau_{load} \tag{4}$$

where J_{SW} is the equivalent moment of inertia of the steering system with respect to the steering wheel, θ_{SW} is the steering angle of the handwheel, τ_1 is the assisting torque with respect to the control conflict between the human driver and machine system, and τ_2 is the steering torque of the driver. τ_{load} is the equivalent steering load, which is composed of the steering system's equivalent viscous friction torque and self-aligning torque. The self-aligning torque is calculated with respect to the steering wheel pneumatic trail in [28]; the calculation of τ_{load} can be expressed as

$$\tau_{load} = B_{SW}\ddot{\theta}_{SW} + \frac{2C_f d_w}{N_s}\left(\delta_f - \frac{v_y + d_p\dot{\varphi}}{v_x}\right) \tag{5}$$

where d_w is the width of the front wheel, d_p is the pneumatic trail of the front wheel, and B_{SW} is the equivalent viscous friction damping coefficient of the steering system.

The steering transmission from the steering wheel angle θ_{SW} to the front wheel steering angle δ_f is assumed as a linear relation. If the transfer ratio is defined as N_s, the relation can be described as $\theta_{SW} = \delta_f N_s$. Substituting Equations (4) and (5) into Equation (1), and denoting the lateral deviation of the vehicle from its starting point as Y , the system state equation of the vehicle dynamic is expressed as

$$\begin{cases} \dot{x} = Ax + B(\tau_1 + \tau_2) \\ y = Cx \end{cases} \tag{6}$$

where

$$\boldsymbol{x} = \begin{bmatrix} \theta_{SW} & \dot{\theta}_{SW} & v_y & \dot{\varphi} & Y & \varphi \end{bmatrix}^T$$

$$\boldsymbol{A} = \begin{bmatrix} 0 & 1 & 0 & 0 & 0 & 0 \\ -\frac{c_1}{N_s} & -\frac{B_{SW}}{JSW} & \frac{2c_1}{v_x} & \frac{2c_1 d_p}{v_x} & 0 & 0 \\ -\frac{2C_f}{m_c N_s} & 0 & c_2 & c_3 - v_x & 0 & 0 \\ -\frac{2l_f C_f}{I_c N_s} & 0 & c_3 & c_4 & 0 & 0 \\ 0 & 0 & 0 & 0 & 0 & v_x \\ 0 & 0 & 0 & 1 & 0 & 0 \end{bmatrix}$$

$$\boldsymbol{B} = \begin{bmatrix} 0 & \frac{1}{J_{SW}} & 0 & 0 & 0 & 0 \end{bmatrix}^T$$

$$\boldsymbol{C} = \begin{bmatrix} 0 & 0 & 0 & 0 & 1 & 0 \\ 0 & 0 & 0 & 0 & 0 & 1 \end{bmatrix}$$

$$c_1 = \frac{2C_f d_w}{N_s J_{SW}} \qquad c_2 = \frac{2C_f + 2C_r}{m_c v_x}$$

$$c_3 = \frac{2l_f C_f - 2l_r C_r}{m_c v_x} \qquad c_4 = \frac{2l_f^2 C_f + 2l_r^2 C_r}{m_c v_x}$$

In order to be used in the continuous control model, the above system state equation needs to be converted to the discrete form with the sampling time T_s. If k is defined as the discrete time instance, the equation can be rewritten as:

$$\begin{cases} x(k+1) = A_d x(k) + B_d(\tau_1 + \tau_2) \\ y(k) = Cx(k) \end{cases} \tag{7}$$

where $A_d = e^{AT_s}$ and $B_d = B\int_0^{T_s} e^{At}\,dt$.

In this paper, the related physical parameters of the above vehicle dynamics model are shown in Table 1.

Table 1. Physical paramete rs of the vehicle dynamics.

Symbol	Description	Value
m_c	Vehicle mass	1406 kg
J_c	Vehicle yaw moment of inertia	1802 kg·m^2
v_x	Vehicle cruising speed	20 m/s
l_f	Distance from vehicle center of gravity to front axle	1.016 m
l_r	Distance from vehicle center of gravity to rear axle	1.562 m
C_f	Cornering stiffness of one single front wheel	70,000 N/rad
C_r	Cornering stiffness of one single rear wheel	50,000 N/rad
J_{SW}	Moment of inertia of steering system	0.1 kg·m^2
B_{SW}	Steering system linear damping coefficient	0.8 Nm·s/rad
N_s	Steering system angle reduction ratio	16
d_w	Width of front wheel	0.2 m
d_p	Front wheel pneumatic trail	0.008 m

2.3. Driver System Modeling

Based on the above discussion, the prediction of the motion generated from the human side is necessary during shared control of the vehicle. The prediction model to describe the driver's lange change maneuver can be divided into two parts: driver's-intent recognition and trajectory prediction.

The driver's-intent recognition model was designed to obtain the driving behaviors from the human, including lane keep (LK), left lane change (LLC), and right lane change (RLC). The relationship between vehicles in contextual traffic is an important reference factor to determine the driving behaviors of humans. To describe the interaction between the controlled vehicle and other surrounding vehicles, this paper defines a lane-change traffic scene as shown in Figure 3. The traffic flow includes the ego vehicle (EV) and obstacle vehicles (OVs). D_i and TG_i are the distances and time gaps between the EV and other surrounding vehicles.

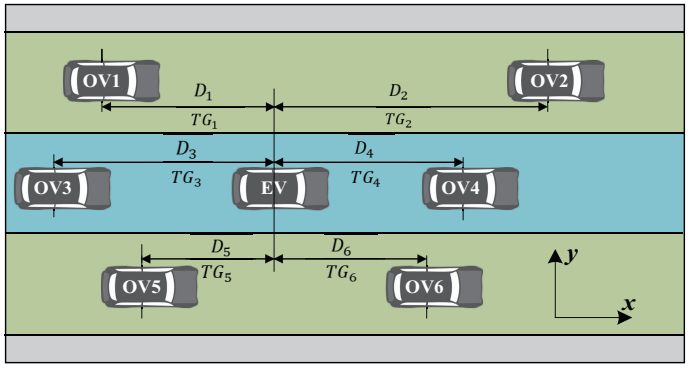

Figure 3. The scene of the traffic flow grid graph.

Based on the traffic information in Figure 3, a long short-term memory (LSTM) network was employed as the driver's-intent recognition model. With a special memory function structure, LSTM algorithm is believed to have an excellent prediction performance for the sequence variables [23]. However, there also exists a shortcoming that limits it to be used in multi-variable and multi-step sequence data, because the model usually transforms the two-dimensional data into one-dimensional data, which will drop some important features. To obtain an accurate prediction for driver behavior in lane change maneuvers, this paper proposes the augmentation of the LSTM algorithm with a convolutional neutral network (LSTM-CNN) for sequences classification.

The structure of the motion prediction model based on the LSTM-CNN model is shown in Figure 4. As shown in Figure 4, the input sequence includes the state variable of the EV and the interactions between the other OVs. The input sequence of the LSTM-CNN model can be expressed as $N_{input} = [y, v_y, TG_i]$, where y and v_y are the lateral position and

lateral velocity of the EV and TG_i is the time gap between the EV and other surrounding vehicles. The output value of the motion prediction model is expressed as N_{output}, which represents three kinds of driver motion behavior: lane keep (LK), left lane change (LLC), and right lane change (RLC). The sequence folding layer with the name "Seq-fold" was used to preprocess the data sequence from N_{iutput}. Furthermore, the convolutional neutral layer with the name "Conv" can restore sequence data and extract the feature. Then, the "Conv" follows the batch normalization (BN) and rectified linear unit (Relu) to improve the generalization and expression ability of the network model. A sequence unfold layer (Seq-unfold) combines the output of the Relu layer and the Seq-fold layer, which is the input of the lstm layer (Lstm). Finally, the fully connected layer (FC) and a softmax layer (Softmax) obtain the prediction result N_{output} via mapping and sorting.

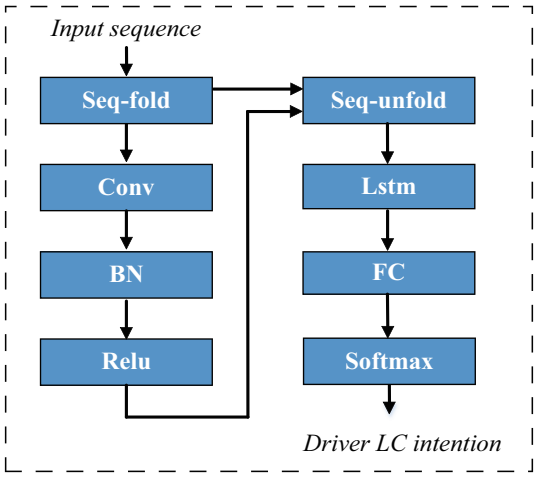

Figure 4. The structure of LSTM-based motion prediction model.

The LSTM-CNN model was trained and tested by the next-generation simulation (NGSIM) dataset, which includes real traffic trajectory data conducted by the United Stated Federal Highway Administration. The NGSIM dataset includes the concrete information for all the vehicles, such as Vehicle ID, Position X, Position Y, Vehicle Speed, Lane ID, and so on. In this paper, we selected 7134 data samples from the NGSIM dataset to train the proposed LSTM-CNN model. The details of the driver's-intent recognition model can be found from our previous literature [29]. By using the time gap information of the ego vehicle in contextual traffic, an improved prediction accuracy with about 90% can be achieved to describe the driver's lane change behavior.

Based on the recognition of driver intention, the trajectory of the lane change maneuver in the short-term future can be predicted. The physics-based prediction method assumes that the vehicle's dynamic parameters are constant in the preview time. The prediction effect of the physical-based methods in a short period of the time needs fewer calculation resources than that of the machine-learning-based methods. Based on the algorithm in [30], here, a constant turn rate and acceleration (CTRA) model was adopted to predict the driver's driving trajectory of the lane change maneuver in the predicted time domain. The state variable of the CTRA model can be expressed as follows:

$$x^{CTRA} = (X,\ Y,\ \varphi, \dot{X},\ \dot{Y},\ \dot{\varphi}) \tag{8}$$

where X and Y mean the vehicle's longitudinal and lateral displacement relative to the world coordinate system, φ is the yaw angle of the vehicle, and $\dot{X}$, $\dot{Y}$, and $\dot{\varphi}$ represent the velocity variables of the vehicle by differentiation, respectively.

If the sampling time is defined as Δt, by iterating from the current step t to the predicted time domain, a set of predictive vehicle states in the limited step N_p is expressed as $x^{CTRA}(t), x^{CTRA}(t+\Delta t), ..., x^{CTRA}(t+N_p\Delta t)$. As shown in Figure 5, the blue segment sequences represent the prediction of driver trajectories in a predetermined time range.

The prediction of the driver's trajectories were achieved with the combination of segment sequences, and the sampling time was set as 0.1 s in this case.

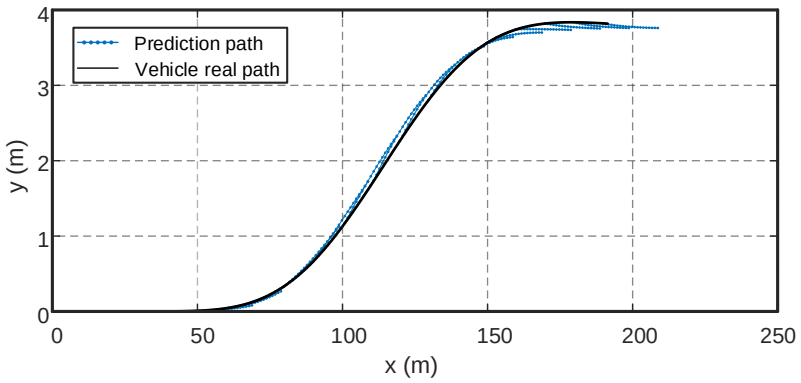

Figure 5. The predicted trajectory segments and the driver's real trajectory.

Based on the predicted trajectory, an assessment model was designed to evaluate the risk level of the driver's behaviors within a predetermined time domain. Time gap (TG) and time to collision (TTC) are widely used for vehicles' risk assessments to avoid collisions. Since the TG shows time headway to the preceding vehicle with more stringent constraints, here, this paper proposes a risk assessment model based on the TG. To evaluate the degree of influence of contextual traffic on the LC maneuver, we define the time gaps between the ego vehicle and the front/rear vehicles as TG_f and TG_r, respectively. Thus, the risk level R of the vehicle trajectory in specific time can be expressed as

$$\begin{aligned} R &= \frac{\alpha_f}{TG_f} + \frac{\alpha_r}{TG_r} \\ TG_f &= \frac{x_f - x_{EV}}{v_{EV}} \\ TG_r &= \frac{x_{EV} - x_r}{v_r} \end{aligned} \tag{9}$$

where α_f and α_r are the risk coefficients for the front and rear vehicles. x_{EV}, x_f, and x_r are the longitudinal position of the ego vehicle, front, and rear vehicles. v_{EV} and v_r are the longitudinal velocity of the ego vehicle and rear vehicle.

By using the prediction segments of the lane change maneuver, the predictive vehicle states $x^{CTRA}(t)$ are substituted into Equation (9). The sum of the driving risk assessment for the driver's behaviors in the predicted time domain can be expressed as:

$$R^* = \sum_{n=0}^{N_p} R(x^{CTRA}(t + n\Delta t)) \tag{10}$$

Here, R^* can show the environmental risk during the lane change maneuver, which is based on the consideration of the TGs for the surrounding vehicles in Figure 3. The traffic vehicles with a larger TG will result in a smaller risk R^*. The driving risk assessment will be employed to take authority allocation between the human driver and machine assistance.

3. Design of Game-Based Shared Control Algorithm

During human–machine interactive steering control, the motion of the vehicle is commanded at the same time from two intelligent agents. The specific shared control process between the machine system and the human driver can be viewed as a series of non-cooperative Nash games [21]. In this type of game, the steering torques from the machine intelligence and the human driver are coupled to generate the final steering action. The machine system and the human driver formulate their own strategies independently, but are aware of each other's actions and their possible impact on the vehicle's movement.

When the prediction time domains of the machine and the driver are defined to have the same length N_p, the cost functions for the torque inputs from both participants at time instance k are given as

$$\begin{aligned} J_1(\tau_1, \tau_2) &= \sum_{j=k}^{k+N_p-1} \| y(j) - y_1(j) \|^2_{Q_1} + \sum_{j=k}^{k+N_p-1} R_1 \tau_1(j)^2 \\ J_2(\tau_1, \tau_2) &= \sum_{j=k}^{k+N_p-1} \| y(j) - y_2(j) \|^2_{Q_2} + \sum_{j=k}^{k+N_p-1} R_2 \tau_2(j)^2 \end{aligned} \tag{11}$$

where $\tau_1(j)$ and $\tau_2(j)$ are the torque input sequences from the machine system and human driver, $y_1(j)$ and $y_2(j)$ are the target planned-path sequences from the machine system and human driver, and $y(j)$ is the synthetic path sequence by the human–machine interaction. $Q_i = diag(q_Y, q_\varphi)$ is the weight coefficient matrix of the lateral displacement and yaw angle tracking error, which corresponds to the tracking performance of the vehicle. R_1 and R_2 are the weight coefficients of the amount of steering torque input corresponding to the machine intelligence and human intelligence.

Here, τ_i^* is defined as the optimized steering torque allocation strategy under Nash equilibrium. Then, a dynamic programming inverse order method is applied for the solution of τ_i^*. Before using the linear quadratic programming algorithm, Equation (11) needs to be converted to its standard format:

$$\tau_i^* = \underset{\tau_i}{\operatorname{argmin}} \left[\sum_{j=k}^{k+N_p-1} \| \tilde{x}(j) \|^2_{\tilde{Q}_i} + \sum_{j=k}^{k+N_p-1} R_i \tau_i(j)^2 \right], i = 1, 2 \tag{12}$$

where $\tilde{x}(j) = \begin{bmatrix} y(j) & L_i(k) \end{bmatrix}^T$ $\quad \tilde{Q}_i = \begin{bmatrix} K_i^T Q_i K_i & -diag(y_i^T Q_i) \\ -diag(Q_i^T y_i) & 0 \end{bmatrix}$

$K_1 = \begin{bmatrix} C & -I_2 & 0_{2\times(2N_p-1)} \end{bmatrix}^T$ $\quad K_2 = \begin{bmatrix} C & 0_{2\times N_p} & -I_2 & 0_{2\times(N_p-1)} \end{bmatrix}^T$

According to Hamilton formalism, the optimal torque input of the participants under Nash equilibrium has the following form:

$$\tau_i^* = -R_i^{-1} \tilde{B}_i^T P_i \tilde{x} \tag{13}$$

We refer to $-R_i^{-1}\tilde{B}_i^T P_i$ as the torque feedback matrix under Nash equilibrium, where $\tilde{B}_i = \begin{bmatrix} B_i & 0 \end{bmatrix}^T$. Matrix P_i is obtained by solving a series of discrete Riccati equations:

$$\begin{aligned} &P_i = P_i^0 \\ &P_i^{k-1} = P_i^k + T_s[\left(\tilde{A}^k - S_{3-i}^k P_{3-i}^k\right)^T P_i^k + P_i^k \left(\tilde{A}^k - S_{3-i}^k P_{3-i}^k\right) - P_i^k S_i^k P_i^k + \tilde{Q}_i^k] \\ &S_i^k = \tilde{B}_i R_i^{-1} \tilde{B}_i^T \\ &P_i^{N_p} = 0 \end{aligned} \tag{14}$$

During the solution of the above algorithm, the iterative calculation of $P_i^{N_p}$ is started with the initial value as zero. Based on the value of P_i^k, P_i^{k-1} can be derived using the forward iterative calculation. By using the rolling optimization approach, the results of τ_i^* can be recalculated in each computing cycle.

The game-based functions in Equation (12) describe the torque interactions between the machine system and human driver. It can be observed from the cost function that the larger Q_i/R_i is, the more attention the participant pays to the path tracking accuracy. Since R_1 and R_2 are the weight coefficients of the amount of steering torque input corresponding to the machine intelligence and human intelligence, the allocation of shared steering control can be conducted via the adjusting of the related weight coefficient. As illustrated

in [18], in the non-cooperative game model, the penalty coefficients R_1 and R_2 have a significant effect on the performance of the vehicle's lateral movement. The dynamic authority allocation strategy of the game theory is based on the driving risk assessment and human–machine interaction. Here, the relation of two penalty coefficients can be expressed as:

$$R_1 = \mu(K)R_2 \tag{15}$$

where K is the dynamic authority allocation coefficient and $\mu(K)$ is the nonlinear fitting function of K.

Based on the ego vehicle's risk assessment, the machine intelligence compensates the human driver's control input to reduce unsafe driving actions. Since the control strategies of machine intelligence cannot cover all possible driving scenarios, a human-oriented mode is necessary to consider to return final control right to the driver. To describe the conflict between the two participants, the dot product of the torques from the human driver and machine system can be accumulated to show the degree of conflict β.

$$\beta^* = \beta_0 \left[\sum_{j=k}^{N_p+k-1} \tau_1 \cdot \tau_2 \right] \tag{16}$$

where β_0 is the gain coefficient of integral accumulation. An increased cumulative quantity of the steering torques represents a high intervention from the human driver, which is also used to recognize the degree of driving attention. The machine system can reduce unnecessary assistance to follow the driving intention of the human driver. This kind of adaptive game control strategy can achieve a dynamic authority distribution by considering both driving comfort and safety.

Based on the above analysis of human–machine interactions, the shared control strategy can be designed using the driver torque and the ego vehicle's risk assessment. Here, the design of the nonlinear fitting function of $\mu(K)$ in Equation (15) is calculated using a fuzzy logic controller. The fuzzy control method is widely used in many studies because the control process can be smoother and more effective. Moreover, the fuzzy control method can integrate expert experience and make parameter design more flexible.

The fuzzy controller has two input variables, such as the degree of conflict β^* and a comprehensive driver's risk assessment R^*, and one output is the dynamic authority allocation coefficient K. The fuzzification of these variables employed five associated linguistic values: very small (VS), small (S), medium (M), big (B), and very big (VB). The fuzzy rules were generated based on a substantial amount of simulation experience, which had a basic principle: the more hazardous the ego vehicle's situation and the smaller the driver torque, the higher the dynamic authority allocation coefficient. With regard to the above fuzzy logic, the fuzzy surface of the game-based shared controller is shown in Figure 6.

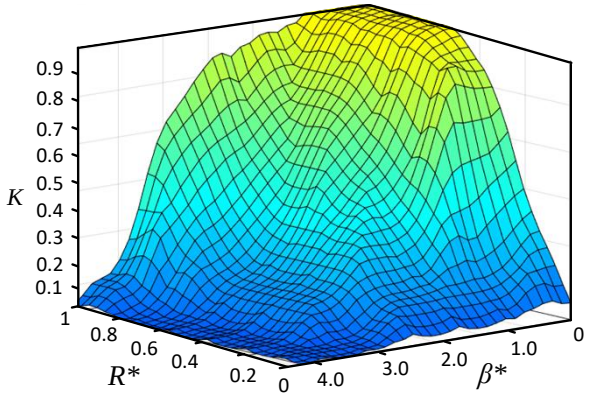

Figure 6. Fuzzy surface of the shared controller.

4. Experiments and Analysis

In order to verify the performance of game-based shared steering control, hardware-in-the-loop (HIL) experiments were conducted on a self-developed driving simulator. The structure of the experimental platform for a steer-by-wire system is shown in Figure 7. The steering-assisted motor on the handwheel module is used to generate control torque from the machine intelligent system. The handwheel angle and torque signals are collected by installed sensors. The real-time control is conducted by a rapid control prototype dSPACE PX20. The game-based algorithmic model was built under MATLAB/Simulink environment. The related parameters of shared control algorithm are shown in Table 2. The sampling rate of the system was selected as 10 ms. CAN bus communication was applied between the handwheel module and the real-time controller. To simulate a human–machine interaction progress, traffic scenarios with vehicle dynamic models were constructed in the automotive simulation environment.

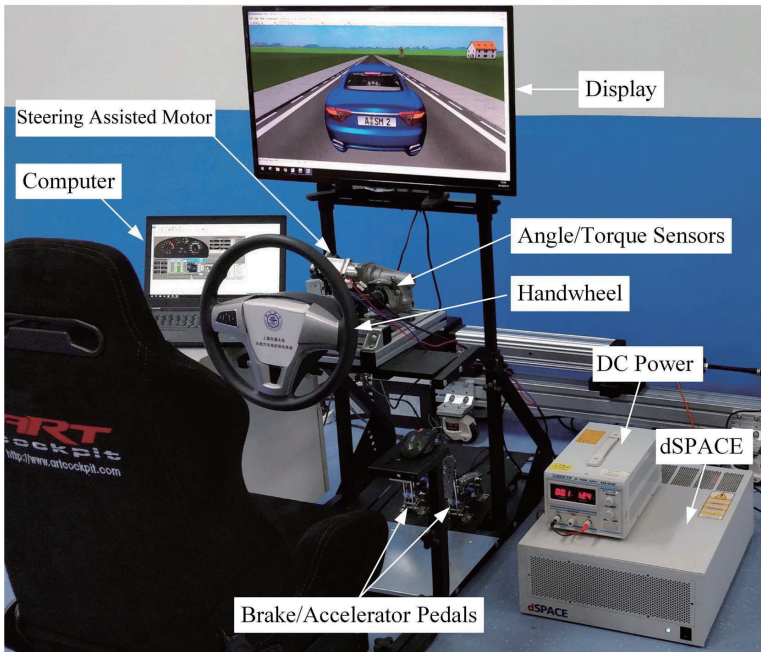

Figure 7. Hardware-in-the-loop platform of shared steering control.

Table 2. Parameters of adaptive shared control strategy.

Symbol	Description	Value
N_p	Control prediction time domain length	20
$a_{y,max}$	Upper limit of lateral acceleration value	2 m/s^2
α_f	Weighting factor for the evaluation of risk level	1.5
α_b	Weighting factor for the evaluation of risk level	1.1
β_0	Weight coefficient for the degree of conflict	0.01

Based on the degree of consistency of the control inputs from the human driver and machine system, different traffic scenarios were designed to show the efficiency of the proposed game-based shared steering algorithm. The test was conducted on the previously mentioned HIL experimental platform. The performance of shared control with a consistent human–machine goal and conflicting goal were analyzed in the lane changing scenarios.

In order to further verify the performance of the proposed strategy, the benefits of the proposed shared control strategy against other methods are discussed. In each of the following experimental scenarios, the proposed method with adaptive game parameters is analyzed by comparing the control results with the conventional game-based assistance with the fixed parameters in [19].

The tests on the HIL experimental platform were conducted with different human drivers. We recruited six volunteers to take shared steering control in a lane change environment. These six human drivers were completely familiarized with the driving simulator through at least 10 driving tests. During the experiment, a predefined route for lane changing was drawn in the simulated environment for the reference of the human driver. In order to reveal the driver's effort during the shared steering control, we used an index DE to denote the steering burden of the driver. Moreover, another index LA was defined to denote the comfort and safety during lane change control. Here, the values of DE and LA are evaluated by using the average of all participants' results. If the total time step for lane changes is set as n, these indexes are calculated by

$$\begin{aligned} DE &= \sqrt{\frac{\sum_{i=0}^{n} {\tau_2}^2}{n}} \\ LA &= \sqrt{\frac{\sum_{i=0}^{n} {a_y}^2}{n}} \end{aligned} \tag{17}$$

In this paper, the steering behavior of the human driver was performed under limit-handling conditions to reduce the influence of psychological factors. Therefore, the target paths were predefined to validate the proposed control model, which are shown in Figure 8. The road to traverse on was configured as a straight lane with the controlled vehicle starting from the left side, and a single static obstacle was located in front of the vehicle. Based on the state of the driver's attention, three kinds of lane changing scenarios with different driver target paths were analyzed to show the effect of shared steering control. Case 1 is a cooperative scenario where the driver makes an earlier collision avoidance than the machine's planning. Case 2 is a cooperative scenario where the driver makes a later collision avoidance than the machine's planning. The control effect from the machine was minimized in the first case to reduce the interference, and increased in the second case to correct the driver's later action. Case 3 is a conflict scenario where the driver resists against the lane change by keeping forward driving behavior. This scenario was used to verify the return of final control to the human driver if the human does not trust the machine's decision.

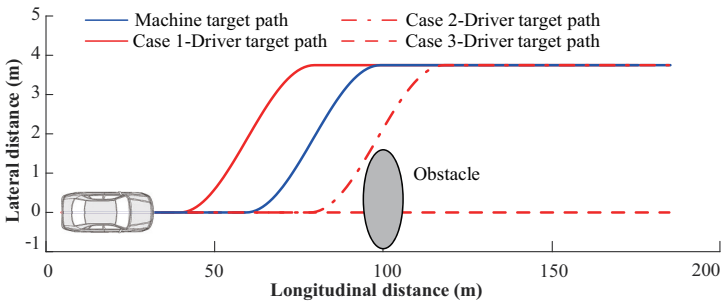

Figure 8. Target paths of machine and driver in the lane changing scenarios.

In this lane changing scenario, the vehicle was driving with constant longitudinal velocity from the beginning of experiment. From the general automobile safety standard, a safe distance is not less than 30 m if the vehicle is driving with a speed of 40 km/h [17]. Here, the velocity of the simulated vehicle was set as 40 km/h. The driver was assumed to notice the danger at a 40 m longitudinal position before the obstacle and perform an early lane change motion to promptly avoid the obstacles. Meanwhile, the machine intelligent system was assumed to take avoidance action at a 60 m longitudinal position before the obstacle. The proposed adaptive game-based shared steering control is compared with a previous shared control approach with fixed game parameters. The simulation result is

shown in Figure 9. X is the longitudinal distance and Y is the lateral distance of the lane change trajectory.

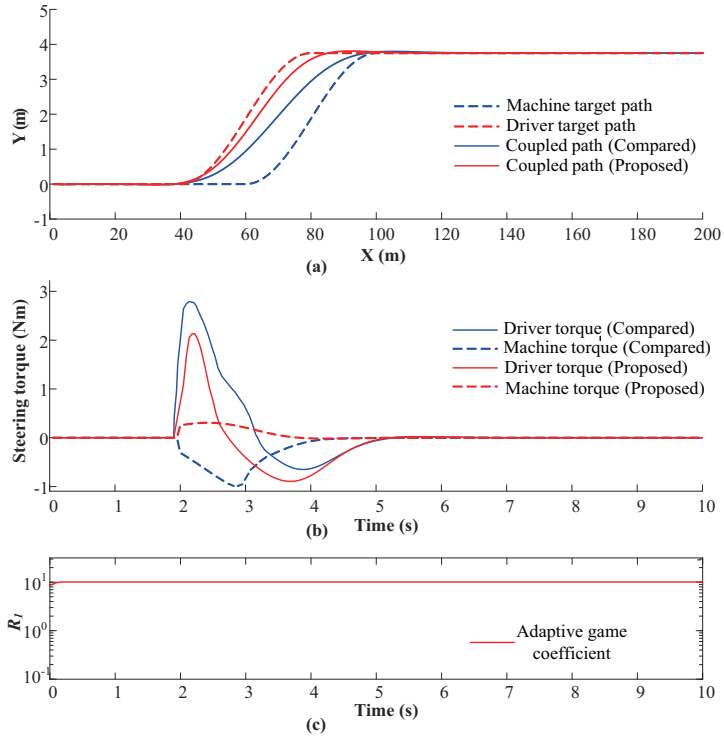

Figure 9. Experimental result when driver makes a timely response to avoid obstacle. (**a**) Driving trajectories with different control methods; (**b**) Steering torque efforts of human and machine; (**c**) Control of adaptive game coefficient.

4.1. Case 1: Scenario with Early Collision Avoidance

Since the target path of the driver is different from that of the machine's planning, it can be found from Figure 9 that the human driver makes a timely lane change to avoid the obstacle in advance. The synthetic path by the compared method is a compromise result, where the vehicle runs along a neutral trajectory between two target paths. Since the prediction of the human driver is a safe action, the synthetic path by the proposed method can achieve a human-oriented result to reduce the intervention from the machine system. The steering torque shows the conflict of the driver and machine system. The proposed method has a smaller steering torque, which is a benefit of the adaptive game-based shared control.

From Figure 10a, the driver's effort index DE and comfort index LA were employed to evaluate the performance of shared steering control. These indexes were calculated using Equation (17). Lateral acceleration and driver steering torque can be used to show the smoothness and comfort during the avoidance motion. To analyze the conflict of steering torques from the human driver and machine system, the coverage ratio of the torque conflict and torque assistance are shown in Figure 10b. It can be found that the proposed method can reduce the conflict of steering torques from the two participants, which brings an improved driving experience.

4.2. Case 2: Scenario with Late Collision Avoidance

The design of this lane changing scenario is similar to that of Case 1. To avoid the static obstacle located in front of the driving vehicle, the machine system was still assumed to take avoidance action at a 60 m longitudinal position before the obstacle. The difference was that the driver was assumed to take a later action due to the inattention of the human. The driver's target path for the lane change was started at an 80 m longitudinal position

before the obstacle, where it was difficult to conduct the available behavior to avoid the obstacle. Here, the shared control model was employed to correct the unsafe behavior of the driver. The simulation result is shown in Figure 11.

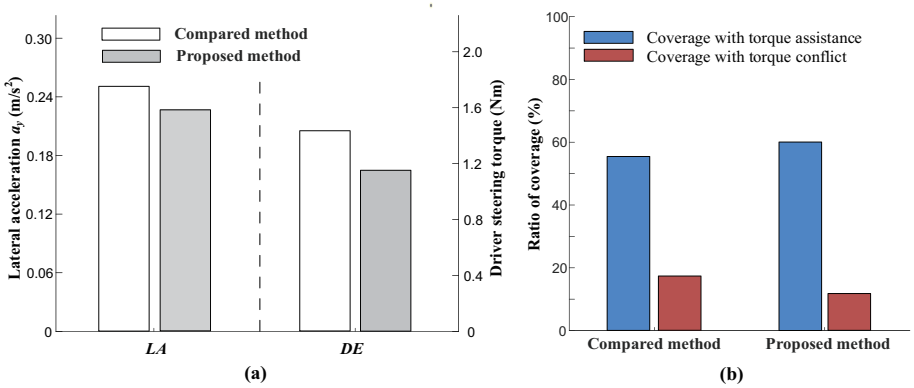

Figure 10. Performance analysis of different control approaches. (**a**) Evaluation indexes of shared steering control; (**b**) Coverage ratio of torque assistance and conflict.

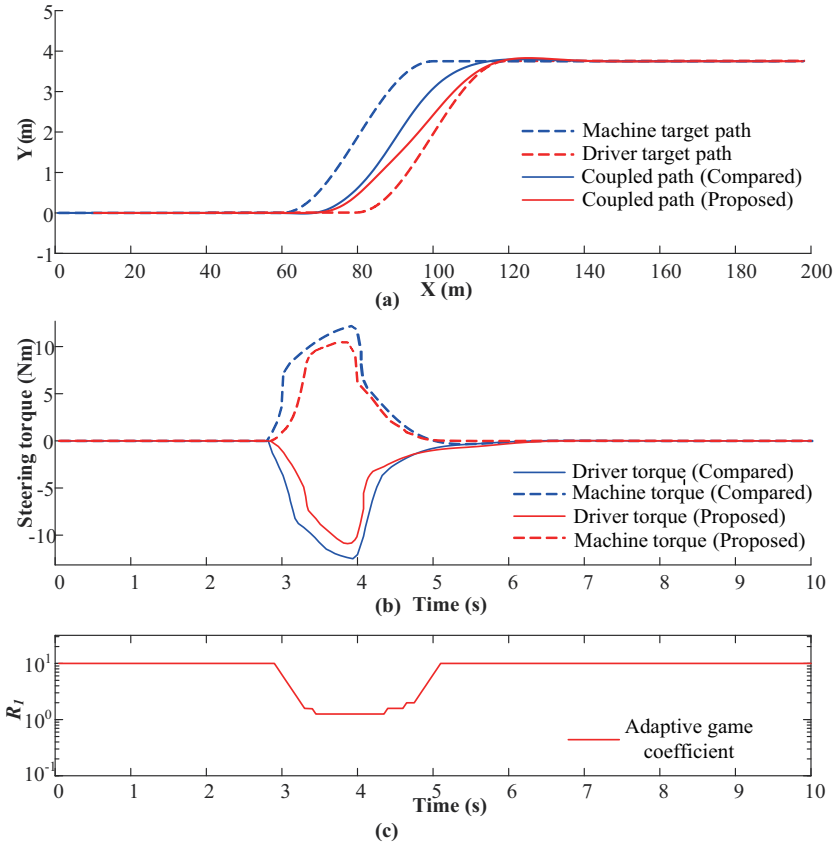

Figure 11. Experimental result when driver makes a late response to avoid obstacle. (**a**) Driving trajectories with different control methods; (**b**) Steering torque efforts of human and machine; (**c**) Control of adaptive game coefficient.

From the experimental results in Figure 11, it can be found that synthetic paths to avoid obstacles were achieved with the assistance of shared control between the human driver and machine system. The authority distribution parameter of game controller R_1 was adjusted to balance the requirements from the two participants. Based on the adaptive game control strategy in Equation (16), the value of R_1 was reduced to increase the authority distribution of machine assistance. Since the compared method was conducted with a fixed

game parameter R_1, the synthetic path was a compromise result with more serious torque conflict. From the evaluation results of lateral acceleration and driver steering torque in Figure 12, the proposed game controller with adaptive parameters had a better performance. The proposed controller can save more than 30% of the steering effort compared with the previous strategy used in the comparison.

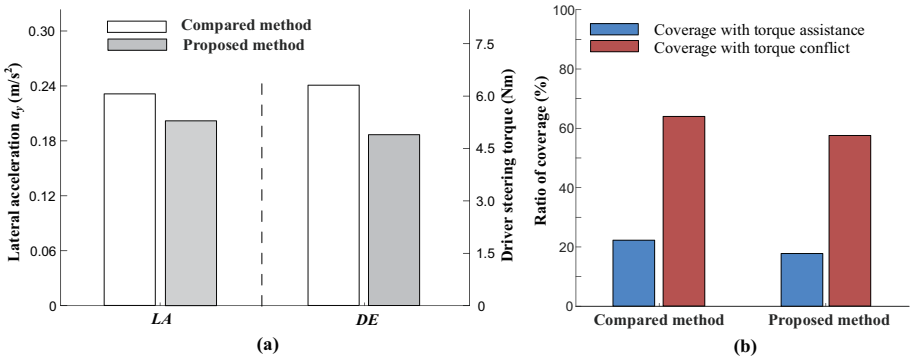

Figure 12. Performance analysis of different control approaches. (**a**) Evaluation indexes of shared steering control; (**b**) Coverage ratio of torque assistance and conflict.

4.3. Case 3: Scenario with Human–Machine Conflicting Goals

The attention of human driver can be easily focused again after being reminded, but the machine system will not discover its inappropriate decision under complex situations, such as the driverless dilemma in [27] and the incorrect detection of the sensory system in [31]. In this scenario, based on the different understandings of the complex traffic environment, the human driver and machine system were assumed to have conflicting driving goals. The target path of the human driver was a straight driving line along the road, and the target path of the machine system was a lane change motion to avoid an obstacle. The driver was arranged to maintain the original forward driving and resist the assistance from the machine system. The experimental result is shown in Figure 13. With the proposed adaptive shared steering algorithm, a human-oriented game control can be realized by considering the real intention of the human driver. This kind of adaptive shared control framework has a human-oriented characteristic during the solution of decision conflict.

Based on the degree of conflict between the two participants, an adaptive game parameter R_1 was adjusted according to the intentional action of the human driver. The intention of the driver was identified by the cumulative amplitude of the steering torque. From the result in Figure 13, it can be found that the synthetic path is returned to a straight driving line after a period of struggle. The synthetic path by the compared method is a compromise path which cannot achieve a flexible shared control in accordance with the driver's intention. From the evaluation results of the lateral acceleration and driver steering torque in Figure 14a, the proposed game controller with adaptive parameter has a better control smoothness and comfort than the compared method. From the compared results in Figure 14b, the coverage ratio of the torque conflict was reduced significantly. The compared method with a machine-oriented control framework cannot pay enough attention to the driver's reaction. The proposed adaptive game approach can avoid single machine-oriented control results, in which the driver can play a dominant role after the recovery of human attention.

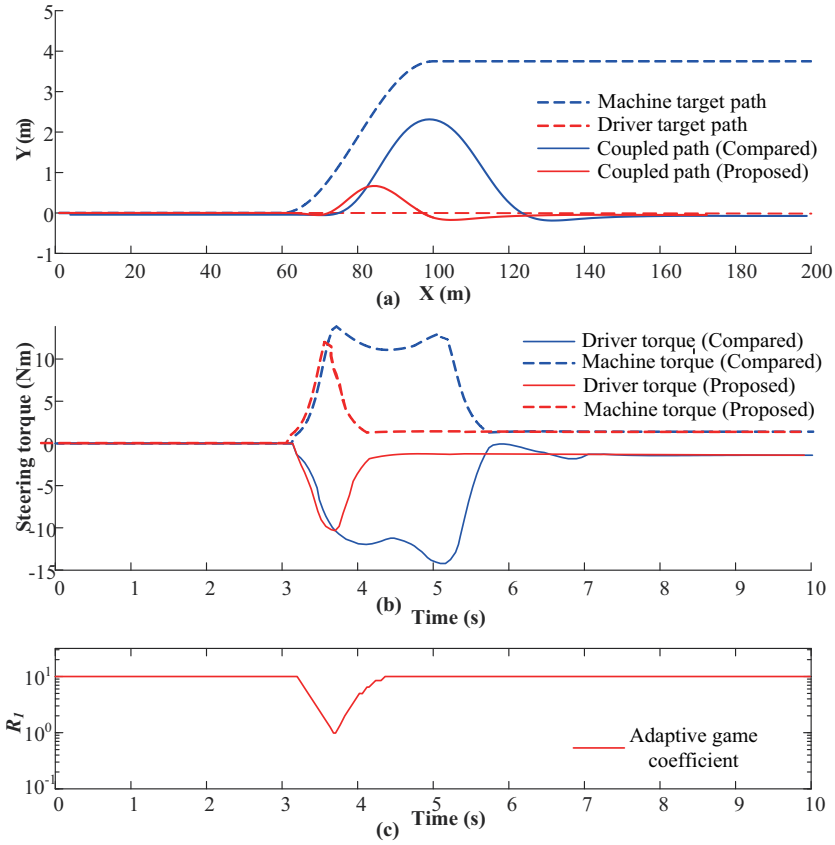

Figure 13. Experimental result when driver deliberately resists the assistance from machine system. (**a**) Driving trajectories with different control methods; (**b**) Steering torque efforts of human and machine; (**c**) Control of adaptive game coefficient.

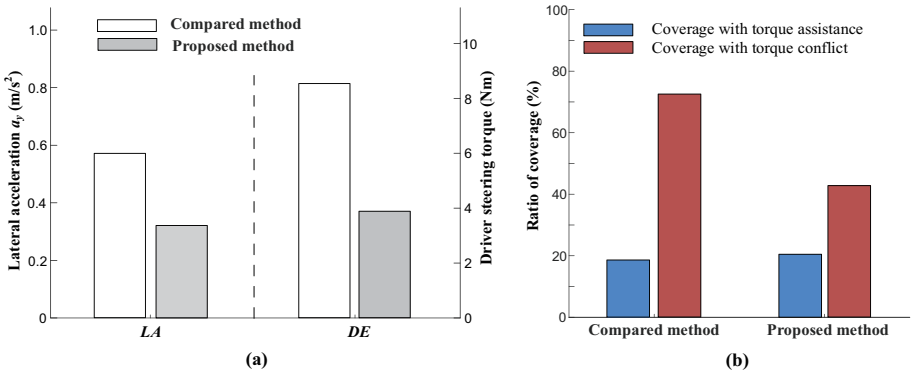

Figure 14. Performance analysis of different control approaches. (**a**) Evaluation indexes of shared steering control; (**b**) Coverage ratio of torque assistance and conflict.

5. Conclusions

In this paper, a game-based shared steering control framework is built to have a flexible human–machine interaction mechanism. Different from previous studies, the prediction of the motion generated from the human driver is integrated into the shared steering control based on the LSTM-CNN model. In addition, the Nash equilibrium solution is derived using the optimum control method. Compared with previous works, an adaptive weighting matrix for the game solution is proposed to pay enough attention to the driver's reaction. The performance of game-based shared steering control is verified with HIL experiments. From the results of different traffic scenarios, the proposed algorithm has benefits to simultaneously enhance driving safety and reduce the degree of conflicts. Moreover,

the proposed adaptive game approach can avoid single machine-oriented control results, in which the driver can play a dominant role after the recovery of human attention.

The shared steering control in this paper is focused on the lateral performance in a predefined driving environment. The driving targets of the human driver and machine system can be predicted using a numerical model. However, the controlled vehicle in real situations with nonlinear and dynamic disturbances is difficult to have accurate prediction results. Game-based control theory has a high requirement for the complete information from each participant. How to improve the robustness of the shared control framework is still an unsolved issue for our future study.

Author Contributions: Conceptualization, C.S. and L.Y.; methodology, C.S. and L.Y.; writing—original draft preparation, X.W.; writing—review and editing, X.W. All authors have read and agreed to the published version of this manuscript.

Funding: This research was supported in part by the National Natural Science Foundation of China (Grant No. 51775331).

Data Availability Statement: Not applicable.

Acknowledgments: The authors would like to thank the National Science Foundation of China for supporting this work.

Conflicts of Interest: The authors declare no conflict of interest.

References

1. Galvani, M. History and future of driver assistance. *IEEE Instrum. Meas. Mag.* **2019**, *22*, 11–16. [CrossRef]
2. Li, L.; Wen, D.; Zheng, N.N.; Shen, L.C. Cognitive Cars: A New Frontier for ADAS Research. *IEEE Trans. Intell. Transp. Syst.* **2012**, *13*, 395–407. [CrossRef]
3. Jing, C.; Shu, H.; Shu, R.; Song, Y. Integrated control of electric vehicles based on active front steering and model predictive control. *Control Eng. Pract.* **2022**, *121*, 105066. [CrossRef]
4. Hu, Y.; Ting, Q.U.; Liu, J.; Shi, Z.Q.; Zhu, B.; Cao, D.P.; Chen, H. Human-machine cooperative control of intelligent vehicle: Recent developments and future perspectives. *Acta Autom. Sin.* **2019**, *45*, 1261–1280.
5. Ding, F.; Shan, H.; Han, X.; Jiang, C.; Peng, C.; Liu, J. Security-Based Resilient Triggered Output Feedback Lane Keeping Control for Human–Machine Cooperative Steering Intelligent Heavy Truck Under Denial-of-Service Attacks. *IEEE Trans. Fuzzy Syst.* **2023**, *31*, 2264–2276. [CrossRef]
6. De Winter, J.C.F.; Petermeijer, S.M.; Abbink, D.A. Shared control versus traded control in driving: A debate around automation pitfalls. *Ergonomics* **2022**, 1–27. [CrossRef]
7. Tan, D.; Chen, W.; Wang, H.; Gao, Z. Shared control for lane departure prevention based on the safe envelope of steering wheel angle. *Control Eng. Pract.* **2017**, *64*, 15–26. [CrossRef]
8. Han, J.; Zhao, J.; Zhu, B.; Song, D. Adaptive Steering Torque Coupling Framework Considering Conflict Resolution for Human-Machine Shared Driving, *IEEE Trans. Intell. Transp. Syst.* **2022**, *23*, 10983–10995. [CrossRef]
9. Li, R.; Li, Y.; Li, S.E.; Zhang, C.; Burdet, E.; Cheng, B. Indirect Shared Control for Cooperative Driving Between Driver and Automation in Steer-by-Wire Vehicles. *IEEE Trans. Intell. Transp. Syst.* **2021**, *22*, 7826–7836. [CrossRef]
10. Tian, Y.; Zhao, Y.; Shi, Y.; Cao, X.; Yu, D.L. The indirect shared steering control under double loop structure of driver and automation. *IEEE/CAA J. Autom. Sin.* **2020**, *7*, 1403–1416. [CrossRef]
11. Brandt, T.; Sattel, T.; Bohm, M. Combining haptic human-machine interaction with predictive path planning for lane-keeping and collision avoidance systems. Intelligent Vehicles Symposium. In Proceedings of the 2007 IEEE Intelligent Vehicles Symposium, IEEE, Istanbul, Turkey, 13–15 June 2007; pp. 582–587.
12. Sentouh, C.; Nguyen, A.T.; Benloucif, M.A.; Popieul, J.C. Driver-Automation Cooperation Oriented Approach for Shared Control of Lane Keeping Assist Systems. *IEEE Trans. Control Syst. Technol.* **2019**, *27*, 1962–1978. [CrossRef]
13. Guo, C.; Sentouh, C.; Popieul, J.C.; Haué, J.B. Predictive shared steering control for driver override in automated driving: A simulator study. *Transp. Res. Part F Traffic Psychol. Behav.* **2019**, *61*, 326–336. [CrossRef]
14. Canale, M.; Fagiano, L.; Signorile, M.C. A model predictive control approach to vehicle yaw control using identified models. *Proc. Inst. Mech. Eng. D J. Automob. Eng.* **2011**, *225*, 1475–1486. [CrossRef]
15. Falcone, P.; Tseng, H.E.; Borrelli, F.; Asgari, J.; Hrovat, D. MPC-based yaw and lateral stabilization via active front steering and braking. *Veh. Syst. Dyn. Suppl.* **2008**, *46*, 611–628. [CrossRef]
16. Cole, D.J.; Pick, A.J.; Odhams, A.M.C. Predictive and linear quadratic methods for potential application to modelling driver steering control. *Veh. Syst. Dyn.* **2006**, *44*, 259–284. [CrossRef]
17. Ji, X.; Yang, K.; Na, X.; Lv, C.; Liu, Y.; Liu, Y. Feedback Game-based Shared Control Scheme Design for Emergency Collision Avoidance: A Fuzzy-LQR Approach. *J. Dyn. Syst. Meas. Control* **2019**, *141*, 081005. [CrossRef]

18. Ji, X.; Yang, K.; Na, X.; Lv, C.; Liu, Y. Shared Steering Torque Control for Lane Change Assistance: A Stochastic Game-Theoretic Approach. *IEEE Trans. Ind. Electron.* **2019**, *66*, 3093–3105. [CrossRef]
19. Flad, M.; Fröhlich, L.; Hohmann, S. Cooperative shared control driver assistance systems based on motion primitives and differential games. *IEEE Trans. Hum.-Mach. Syst.* **2014**, *47*, 711–722. [CrossRef]
20. Ludwig, J.; Gote, C.; Flad, M.; Hohmann, S. Cooperative dynamic vehicle control allocation using time-variant differential games. In Proceedings of the 2017 IEEE International Conference on Systems, Man and Cybernetics, IEEE, Banff, AB, Canada, 5–8 October 2017.
21. Na, X.; Cole, D.J. Linear quadratic game and non-cooperative predictive methods for potential application to modelling driver-AFS interactive steering control. *Veh. Syst. Dyn.* **2013**, *51*, 165–198. [CrossRef]
22. Na, X.; Cole, D.J. Game-theoretic modeling of the steering interaction between a human driver and a vehicle collision avoidance controller. *IEEE Trans. Hum.-Mach. Syst.* **2015**, *45*, 25–38. [CrossRef]
23. Ma, B.; Liu, Y.; Na, X.; Liu, Y.; Yang, Y. A shared steering controller design based on steer-by-wire system considering human-machine goal consistency. *J. Frankl. Inst.* **2019**, *356*, 4397–4419. [CrossRef]
24. Li, M.; Song, X.; Cao, H.; Wang, J.; Huang, Y.; Hu, C.; Wang, H. Shared Control with a Novel Dynamic Authority Allocation Strategy Based on Game theory and Driving Safety Field. *Mech. Syst. Signal Process.* **2019**, *124*, 199–216. [CrossRef]
25. Marcano, M.; Díaz, S.; Pérez, J.; Irigoyen, E. A Review of Shared Control for Automated Vehicles: Theory and Applications. *IEEE Trans. Hum.-Mach. Syst.* **2020**, *50*, 475–491. [CrossRef]
26. Wu, X.; Zhang, M.; Xu, M. Active Tracking Control for Steer-by-Wire System With Disturbance Observer. *IEEE Trans. Veh. Technol.* **2019**, *68*, 5483–5493. [CrossRef]
27. Greene, J.D. Our driverless dilemma. *Science* **2016**, *352*, 1514–1515. [CrossRef] [PubMed]
28. Balachandran, A.; Gerdes, J.C. Designing Steering Feel for Steer-by-Wire Vehicles Using Objective Measures. *IEEE/ASME Trans. Mechatron.* **2014**, *20*, 373–383. [CrossRef]
29. Wu, X.; Yan, L.; Li, H.; Su, C. Forward collision warning system using multi-modal trajectory prediction of the intelligent vehicle. *Proc. Inst. Mech. Eng. Part J. Automob. Eng.* **2022**. [CrossRef]
30. Xie, G.; Gao, H.; Qian, L.; Huang, B.; Li, K.; Wang, J. Vehicle Trajectory Prediction by Integrating Physics- and Maneuver-Based Approaches Using Interactive Multiple Models. *IEEE Trans. Ind. Electron.* **2018**, *65*, 5999–6008. [CrossRef]
31. Burdziakowski, P. Sensors and Sensor's Fusion in Autonomous Vehicles. *Sensors* **2021**, *21*, 6586.

Disclaimer/Publisher's Note: The statements, opinions and data contained in all publications are solely those of the individual author(s) and contributor(s) and not of MDPI and/or the editor(s). MDPI and/or the editor(s) disclaim responsibility for any injury to people or property resulting from any ideas, methods, instructions or products referred to in the content.